5th International Conference
"Computational Mechanics and Virtual Engineering "
COMEC 2013
24- 25 October 2013, Braşov, Romania

ON THE OPTIMIZATION OF THREE-DIMENSIONAL LINE CONTACTS INCLUDING SKEW AND MISALIGNMENT ANGLES FOR CAM-FOLLOWER TYPE CONTACTS

Gabriel Popescu [1]
[1] Department of Mechanical Engineering, Mechatronics and Robotics
Faculty of Mechanical Engineering
Technical University "Gheorghe Asachi" of Iasi, Romania
gpopescu65@yahoo.com

Abstract: *The author presents a fast and accurate method to find the "optimum" pressure distribution in case of non-hertzian elastic contact problems in line contacts. This kind of analysis requires a complete three-dimensional investigation due to the finite length of the contacting bodies. A general elastic contact solver is presented first, followed by a method for a uniform pressure distribution between the contacting elements. Finally, the optimization process is analyzed by comparing the case of possible misalignment and/or tilting angles due to operating conditions, with the original linear profile.*
Keywords: *three-dimensional line contact, skew, misalignment, optimization*

1. INTRODUCTION

The only existing approach that accounts for both the non-hertzian aspect and contact angles is the direct numerical solution of contact problems. Therefore, the analysis must be performed in order to obtain "the real" contact pressures and to avoid spurious stress concentration. Even in the last years faster numerical solutions were developed, problems can arise in case linear contacts, when the presence of skew and/or misalignment angles changes dramatically the shape of the contact area and the corresponding pressure distribution. Real three-dimensional contact problems require numerical analysis in order to obtain both the true contact area and pressure distribution. Since the contact area cannot be known in advance and has to be obtained together with the positive pressures, in case when the initial chosen contact domain is small than real one, spurious stress concentration arise along the domain border. The contact surface must be extended, and for this reason, a special procedure was developed, in order to deal with the possible presence of skew and/or misalignment angles in line contact problems.

An investigation was carried out in order to develop an algorithm for the fast and true contact pressure distribution. Several cases were investigated and the results are presented.

2. GENERAL CONSIDERATIONS

The Hertz theory assumes that when two bodies are in contact, the profile of each surface in the region close to the origin can be approximately expressed by [1]:

$$z_1 = \frac{x_1^2}{R_{11}} + \frac{y_1^2}{R_{12}} \tag{1}$$

In the above relation, R_{11} and R_{12} are the principal radii of curvature of the surface at the origin.

For the second surface we have:

$$z_2 = -\left(\frac{x_2^2}{R_{21}} + \frac{y_2^2}{R_{22}}\right) \tag{2}$$

The separation between the two surfaces in a common system of coordinates may be written:

$$h = z_1 - z_2 = A \cdot x^2 + B \cdot y^2 = \frac{x^2}{R_1} + \frac{y^2}{R_2} \tag{3}$$

where A and B are positive constants and R_1 and R_2 are defined as the principal relative radii of curvature.

In case of line contacts, the equation (3) cannot fully describe the separation between cylindrical shaped bodies. Usually, the follower's geometry involves several crowning radii and a correction term is needed. Generally, considering and the cams made from several different radii, Natsumeda [2] derived the following relation:

$$h(x,y) = z_1(x_1, y_1) - z_2(x_2, y_2) + d1(x_1) + d2(x_2) \tag{4}$$

where $d1(x_1)$ and $d2(x_2)$ are the crowning profiles.

In the case when the follower is "tilted" (misaligned), the equation (4) becomes:

$$h(x,y) = z_1(x_1, y_1) - z_2(x_2, y_2) + d1(x_1) + d2(x_2) + x_1 \cdot \tan(\beta) \tag{5}$$

The presence of a "skew" angle requires the use of a third coordinates system [1], in which the separation of the bodies can be expressed as:

$$h(x,y) = A \cdot x^2 + B \cdot y^2 + d1(x_1) + d2(x_2) + (x \cdot \cos\theta - y \cdot \sin\theta) \cdot \tan(\beta) \tag{6}$$

where:

$$\begin{cases} A = \frac{1}{4} \cdot \left[\frac{1}{R_{11}} + \frac{1}{R_{21}} \right] - \frac{1}{4} \cdot \sqrt{\frac{1}{R_{11}^2} + \frac{1}{R_{21}^2} + \frac{2 \cdot \cos(2\alpha)}{R_{11} \cdot R_{21}}} & \text{(a)} \\ B = \frac{1}{4} \cdot \left[\frac{1}{R_{11}} + \frac{1}{R_{21}} \right] + \frac{1}{4} \cdot \sqrt{\frac{1}{R_{11}^2} + \frac{1}{R_{21}^2} + \frac{2 \cdot \cos(2\alpha)}{R_{11} \cdot R_{21}}} & \text{(b)} \\ \theta = \frac{1}{2} \cdot \tan^{-1}\left(\frac{\frac{1}{R_{21}} \cdot \sin(2\alpha)}{\frac{1}{R_{11}} + \frac{\cos(2\alpha)}{R_{21}}} \right) & \text{(c)} \end{cases} \tag{7}$$

For an accurate determination of the pressure distribution, the crowning profiles need to be evaluated in their own coordinates systems. When computing the pressures in the common coordinates system, since the curvature radii are much larger than the bodies radii, an acceptable approximation is to consider that $d1(x_1) \approx d1(x)$ and respectively $d2(x_2) \approx d2(x)$.

This is in addition to the fact that the skewing angle is small than ± 1.5°.

If only tilting (misalignment) occurs, then is no need for the third coordinates system, and more, the pressure distribution is symmetric with respect to the x-axis. In case of skewing, the pressure distribution remains symmetric in the common coordinates' system, while in the system attached to cam it becomes anti-symmetric.

In order to assess the influence of the skew angle on the shape of the contact area and corresponding pressure distribution, the analysis must be performed in the coordinates system (x2, y2) attached to the cam. In this case, the initial separation between bodies that can be approximated as cylinders is given by the relation [2]:

$$h(x,y) = \frac{y_1^2}{2 \cdot R_{11}} + \frac{y_2^2}{2 \cdot R_{21}} + d1(x_1) + d2(x_2) + x_1 \cdot \tan(\beta) \tag{8}$$

With proper modification, including the possible presence of a skew angle, the above relation becomes:

$$\begin{aligned} h(x,y) = {} & \frac{(x_2 \cdot \sin\alpha + y_2 \cdot \cos\alpha)^2}{2 \cdot R_{11}} + \frac{y_2^2}{2 \cdot R_{21}} + d1(x_2 \cdot \cos\alpha - y_2 \cdot \sin\alpha) + d2(x_2) + \\ & (x_2 \cdot \cos\alpha - y_2 \cdot \sin\alpha) \cdot \tan(\beta) \end{aligned} \tag{9}$$

It is easy to demonstrate that in case of zero value for the skew angle, the equations (6) and (9) are identical.

3. LINE CONTACTS – SOLUTIONS TO IMPROVE CONTACT GEOMETRY

Various linear profiles were developed and improved to avoid edge loading:

- Linear profile with one crowning radius: So and Gohar [3], Reussner [4], Hartnett [5]
- Circular crowning with large radius: Moyer and Neifert [6], de Mul et al. [7], Torstenfelt et al [8,9]
- ZB type roller with linear profile and two crowning radii at the end
- B-TAN (3 crowning radii) and CIR (2 crowning radii): de Mul [7], Torstenfelt [8,9]

- Logarithmic profile or Lundberg profile [10] and modified Lundberg Profile, Lösche [11]

The best results are obtained with logarithmic profile, but it is not so practical for engineers and manufacturers. Usually, the profiles are optimum for a particular load; changing the load value will require a new profile to minimize the contact pressures.

Several methods can be used to improve contact capacity:

- Minimization of the maximum of the contact pressure
- Maximization of rigid body displacement
- Maximization of torque or contact resultant force between the bodies
- Minimization of frictional power loss
- Optimization of the shape by controlling the contact pressure distribution

In what concern the strength of rolling contacts, numerical static contact simulations show that material microstructure and heat treatment are of major importance. Assuming that rolling contact fatigue is generated by the plasticity phenomena, the maximum contact pressures that allow a bearing to operate under "safe" condition were derived, Popescu et al [12]. The values are given in Table 1 and are in agreement with operating pressures cited by Lorösch [13] and Zwirlein and Schlicht [14], which do not produce subsurface initiated contact fatigue.

Table 1: Maximum operating contact pressures for different bearing steel hardened variants

Material	Contact pressure [MPa]
SAE 52100, martensite + retained austenite (100Cr6)	2550
SAE 52100, martensite	3000
SAE 52100, bainite	3050
16MnCr5, martensite + retained austenite	2200

The proposed solution to obtain a "uniform contact pressure" is given below:

- Step 1: For a known geometry, the load that produces a hertzian contact pressure equal with the maximum operating contact pressure (Pmax) is computed.
- Step 2: For a large number of mesh elements (over 2,000), the elementary contact pressures are calculated by using a combined Conjugate Gradient – Multi-Level-Multi-Solution method [15].
- Step 3: In the contact areas where the pressures are higher than Pmax, the pressure is redistributed along the rolling direction (y) in order to have an elliptical variation from 0 to Pmax, with the corresponding increase of the contact width in that region (parallel strips along rolling direction).
- Step 4: The equilibrium between the applied and effective contact load is checked.
- Step 5: From the difference between contact surface normal displacements based on the initial and modified contact pressures, the follower axial's correction is derived and a new profile made of 2 crowning radii is obtained (the continuity of the profile along the follower length is a necessary condition).
- Steps 2 to 5 are repeated until no change in crowning radii is noticed, for an imposed accuracy (usually 6-7 iterations).

4. EXAMPLE OF THE OPTIMIZATION PROCESS

The following parameters were used:

- Applied load: 8000 (N)
- Follower geometry: linear profile with crowning-end radius of 1 (mm), total length 12 (mm)
- Cam diameter: 40.5 (mm)
- Material: standard 52100 bearing steel (100Cr6)
- Modulus of elasticity: 210 (GPa) and Poisson coefficient: 0.3
- Maximum contact pressure: 2550 (MPa)

Figures 1 and 2 show the initial and final contact pressures, obtained from the above described algorithm, while in figure 3 the difference between roller's original and optimized profile is given. The new profile consists of two circular crowning, very similar to a modified Lundberg profile. Figure 4 presents the axial contact pressures in case of a large load, including possible skew and misalignment of the follower. It can be seen that in all situations, the "optimized" profile has superior performance than the original, with moderate edge stress, below the safety limit.

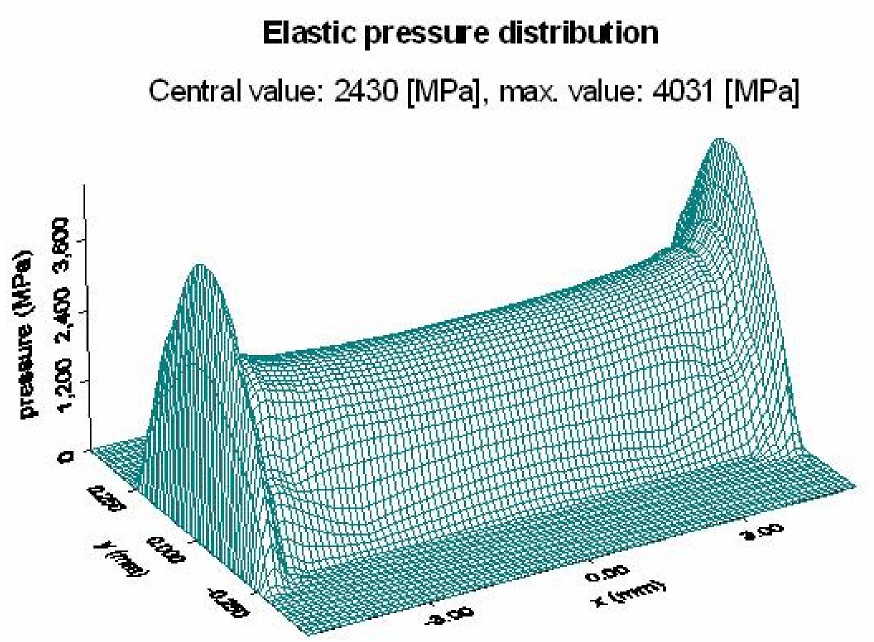

Figure 1: Elastic contact pressures, original geometry

5. CONCLUSION

A general numerical procedure was developed in order to compute the real contact area and pressure distribution in cam-follower contacts, including the possible presence of skew and misalignment angles. The extent of the contact area is more pronounced when misalignment occurs. An optimization process of the follower profile was carried out, starting from the maximum allowable contact pressure that does not initiate sub-surface plasticity. The derived profile shows excellent behavior, even in case of high load, including the possible skew and misalignment of the roller.

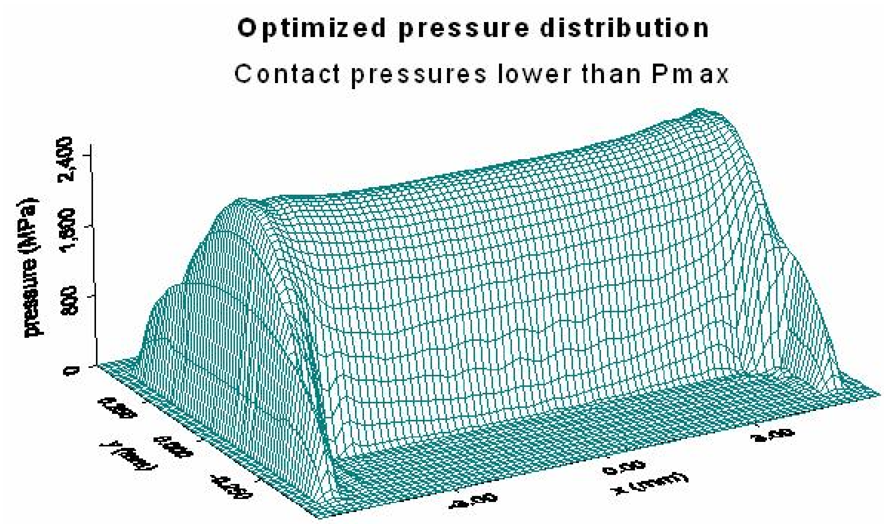

Figure 2: Optimum contact pressures, modified geometry

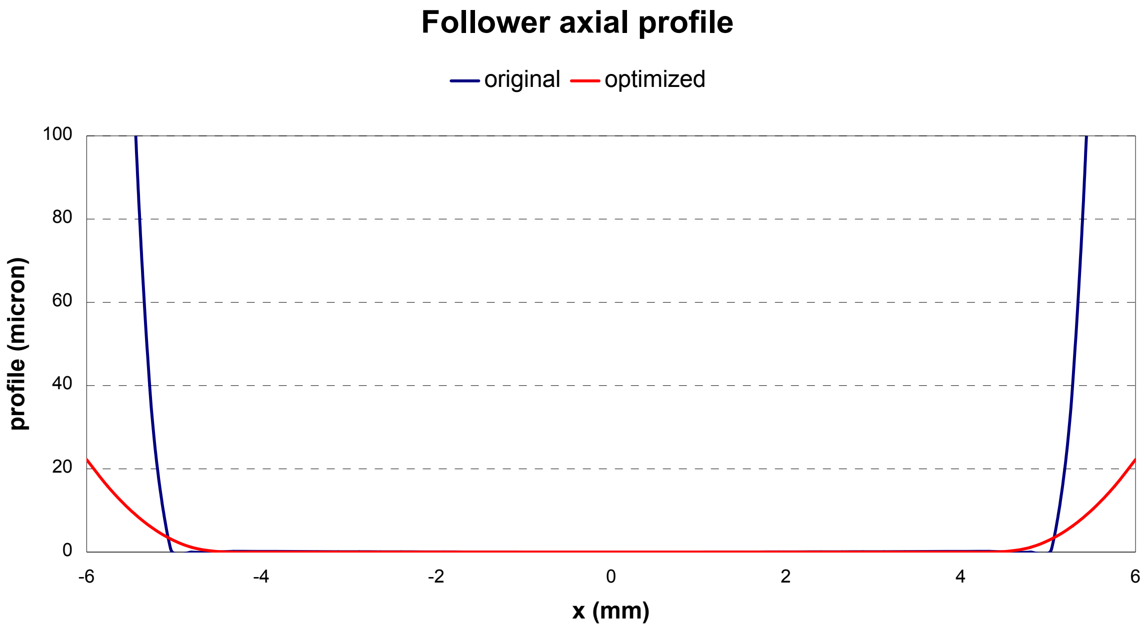

Figure 3: Follower axial profile
ORIGINAL: linear with R_end = 1.0 (mm)
OPTIMIZED: R1 = 51213.9 (mm); 0 to 4.488 [mm]
R2 = 52.2 (mm); 4.488 to 6 (mm)

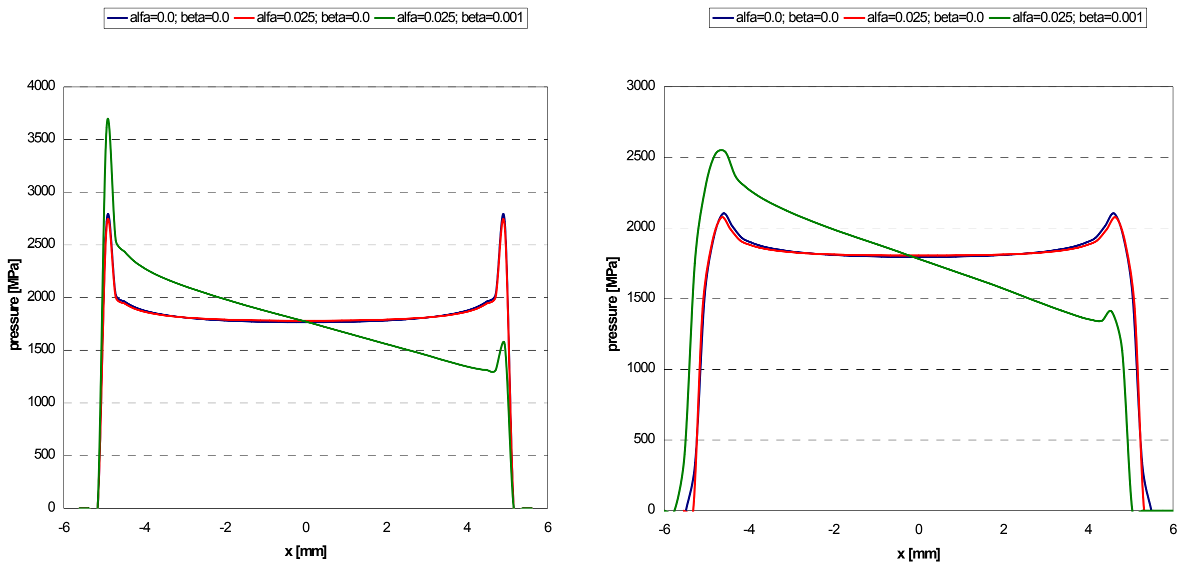

a b

Figure 4: Cam-follower contact pressure distribution
a) original profile, b) optimized profile

REFERENCES

[1] Johnson, K. L. – Contact mechanics, Cambridge University Press, UK, 1985

[2] Natsumeda, S., Application of multi-level multi-integration to contact problems, Part 1: non-hertzian contact in rolling bearings, Proc. Instn. Mech. Engrs., 1999, vol. 123, part J, pp. 63-80

[3] So, H., Gohar, L. – The elastic distortion of rollers under combined radial and thrusts loads, ASME Journal of Lubrication Technology, 1983, vol. 105, pp. 189-197

[4] Reussner, H. - The Logarithmic Roller Profile – Key to Superior Performance of Cylindrical and Taper Roller Bearing, Ball Bearing Journal, 1987, 230, SKF, pp. 2-10

[5] Hartnett, M. J. – The analysis of contact stresses in rolling element bearings, ASME Journal of Lubrication Technology, 1979, vol. 101, pp. 105-109

[6] Moyer, C. A., Neifert, H. R. – A first order solution for the stress concentration present at the end of the roller contact, ASLE Transactions, 1963, 6, pp. 324-336
[7] de Mul, J. M., Kalker, J. J., Fredriksson, B. – The contact between arbitrarily curved bodies of finite dimensions, ASME Journal of Tribology, 1986, vol. 108, pp. 140-148
[8] Torstenfelt, B., Fredriksson, B. – Pressure distribution in crowned roller contacts, Engineering Analysis, 1984, vol. 1, 1, pp. 32-39
[9] Torstenfelt, B. – Contact problems with friction in general purpose finite element computer program, Computers and Structures, 1983, vol. 16, 1-4, pp. 487-493
[10] Lundberg, G. - Elastiche Berührung Zweier Halbraüme, Forschung auf dem Gebiete der Ingenieurwesens, 1939, vol. 10, no. 5, pp. 201-211
[11] Lösche, T. – Capacity increase due to modified line contact in cylindrical and tapered roller bearing, Ball and Roller Bearings Engineering, 1987, vol. 1, pp. 4-9
[12] Popescu, G., Gabelli, A., Morales-Espejel, G. E., Wemekamp, B. – Microplastic material model and residual fields in rolling contacts, Journal of ASTM International (JAI), vol.3, no. 5, May 2006
[13] Lorösch, H.-K. - Influence of Load and Magnitude on the Life Exponent for Rolling Bearings, Rolling Contact Fatigue Testing of Bearing Steels, ASTM STP 771, J. J. C. Hoo, Ed., American Society of Testing and Materials, Philadelphia, PA, 1982, pp. 275-292
[14] Zwirlein, O., Schlicht, H., - Rolling Contact Fatigue Mechanisms-Accelerated Testing Versus Field Performance, Rolling Contact Fatigue Testing of Bearing Steels, ASTM STP 771, J. J. C. Hoo, Ed., American Society of Testing and Materials, Philadelphia, PA, 1982, pp. 358-379
[15] Polonsky, I., Keer, L.M. - A Numerical Method for Solving Rough Contact Problems Based on the Multi-Level Multi-Summation and Conjugate Gradient Techniques, Wear, 231, 1999, pp. 206-219